MATERIALS FOR ELECTRONIC ENGINEERING

Interaction of Electromagnetic Radiation with Magnetically Functionalized CNT Nanocomposite in the Subterahertz Frequency Range

A. Atdaev[a], A. L. Danilyuk[a], V. A. Labunov[a], S. L. Prishchepa[a]*, A. A. Pavlov[b], A. S. Basaev[c], and Yu. P. Shaman[c]

[a] Belarussian State University of Informatics and Radioelectronics, Minsk, 220072 Belarus
[b] INME, RAS, Moscow, 119991 Russia
[c] SMC Technological Center, Moscow, 124498 Russia
* e-mail: prischepa@bsuir.by
Submitted January 22, 2015

Abstract—The interaction of electromagnetic radiation with a magnetically functionalized nanocomposite based on carbon nanotubes (CNTs) is considered using the model of random distribution of ferromagnetic nanoparticles in the carbon matrix characterized by the presence of resistive–inductive–capacitive coupling (contours). The model is based on the representation of the nanocomposite as a system consisting of the CNT matrix, ferromagnetic nanoparticles, and the interfaces between CNTs and nanoparticles. The wide range of possible resonant phenomena caused both by the presence of contours and the properties of the CNT nanocomposite is shown.

Keywords: carbon nanotubes, magnetic nanocomposite, electromagnetic radiation, resonance, magnetic permeability.

DOI: 10.1134/S1063782616130029

INTRODUCTION

Nowadays, magnetic nanocomposites consisting of ferromagnetic nanoparticles distributed in the matrix of another material are the subject of intensive research. The properties of such materials can be controlled by magnetic field, spin-polarized current, or electromagnetic radiation (EMR). A new class of magnetic nanocomposites based on carbon nanotubes (CNTs) [1] is very promising for microwave applications, such as transfer lines, mixers and detectors, polarizers, aerials, and absorbing materials [2–7]. The absorbing properties of a CNT nanocomposite are mainly determined by dielectric losses. However, the introduction of ferromagnetic nanoparticles into the CNT matrix (magnetically functionalized CNTs—MFCNTs) results in increasing absorption of microwave radiation owing to magnetic losses [3, 8, 9].

To predict the absorbing properties of an MFCNT nanocomposite, it is necessary to carry out a wide range of experimental research and develop theoretical methods that take into account various parameters of the material. One of the key problems is to separate the mechanisms of EMR absorption by components of a complex nanocomposite consisting of a carbon matrix, ferromagnetic nanoparticles, and the interfaces between them [3]. In similar complex systems, it is necessary to take into account the properties of each of the three components and the effect of the interfaces between nanoparticles, while the carbon matrix can be taken into account only by numerical simulation of their parameters. In this case, it is important to use real physical values in the studied frequency range.

In this study, we investigated the interaction of EMR with an MFCNT nanocomposite in the frequency range of 20–200 GHz using an earlier developed to describe the microwave properties of MFCNT nanocomposites [3]. The nanocomposite is represented as a distributed system consisting of resistive (R_i), inductive (L_i), and capacitive (C_i) coupling between its individual components. Similar samples can easily be prepared by chemical vapor-phase deposition using $3d$ ferromagnetic metals (Fe, Co, Ni) as catalysts [10].

MODEL

The description of EMR–MFCNT nanocomposite interaction is based on the approach proposed in [3], which was developed to determine the reflection coefficient R and the transmission coefficient T of EMR for the magnetic nanocomposite at frequencies higher than 1 GHz. In this case, both the magnetic
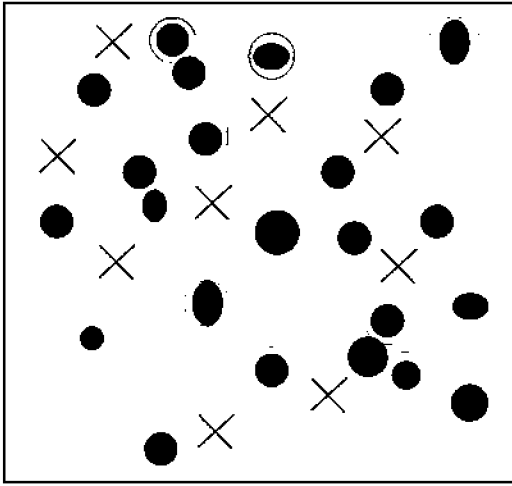
Fig. 1. Schematic representation of MFCNT nanocomposite consisting of CNT matrix (basic background), ferromagnetic particles (black color), shells between nanoparticles and CNT matrix (gray color), and the defects in CNT matrix (daggers). Nanoparticles and defects are randomly distributed in CNT matrix.

properties of nanoparticles and the structural, dielectric, and magnetic properties of the CNT matrix, as well as the transition regions between them, were taken into account. The calculated values of coefficients R and T adequately describe the experimental data for the ranges of X (8—12 GHz) and Ka (26—38 GHz).

In this study, the approach from [3] is developed and the expressions for the magnetic susceptibility and permittivity of the nanocomposite are modified taking into account the possible resistive, capacitive, and inductive coupling between the components of the sample. Indeed, in the frequency range of tens and hundreds of GHz, the microwave properties of the nanocomposite should also considerably depend on the contribution to EMR absorption from the resistive—inductive—capacitive couplings (or contours) arising in such a complex system as an MFCNT nanocomposite, instead of depending only directly on the magnetic and dielectric properties of the material of the CNT matrix and magnetic inclusions. These couplings, caused by the presence of vortex currents in the nanocomposite, are described by the $R_i L_i C_i$ contours.

The MFCNT nanocomposite can be represented as a CNT matrix in which the nanoparticles of a ferromagnetic material are randomly distributed. Each nanoparticle is coated with a protective layer (interface). In addition, the CNT matrix itself is defective. A similar structure of the sample is shown schematically in Fig. 1. The $R_i L_i C_i$ contours are formed mainly due to the resistance of the CNT matrix, the inductance of nanoparticles, and the capacitance of the interface. Under such an assumption, the $R_i L_i C_i$ contours are resonant; i.e., they have a resonance eigenfrequency.

Proceeding from the model described in [3], the following expression is obtained for the magnetic susceptibility of a nanostructure composite:

$$\mu(\omega) = \frac{-B_\mu + \sqrt{B_\mu^2 + 8\mu_1 Q_\mu}}{4Q_\mu}, \tag{1}$$

where the functions

$$B_\mu = \frac{(3 - 5N) - \mu_1 Q_\mu (6 - 7N)}{(3 - 2N)}; \tag{2}$$

$$Q_\mu = \frac{1}{\mu_2} - \frac{i\omega \cdot a\mu_0}{2Z_i(\omega)}; \tag{3}$$

μ_1 and μ_2 are the relative magnetic permeabilities of the CNT matrix and the ferromagnetic nanoparticles, respectively; a is the diameter of nanoparticles; ω is the EMR cyclic frequency; μ_0 is the magnetic constant; N is the bulk concentration of nanoparticles; and Z_i is the impedance of the $R_i L_i C_i$ contour.

For the permittivity, the following expression is obtained:

$$\varepsilon(\omega) = \frac{-B_\varepsilon + \sqrt{B_\varepsilon^2 + 8\varepsilon_1 Q_\varepsilon}}{4Q_\varepsilon} + i(\sigma/\omega), \tag{4}$$

where the functions

$$B_\varepsilon = \frac{(3 - 5N) - \varepsilon_1 Q_\varepsilon (6 - 7N)}{(3 - 2N)}; \tag{5}$$

$$Q_\varepsilon = \frac{Z_i \omega \cdot a\varepsilon_0}{Z_i \omega \cdot a\varepsilon_0 \varepsilon_2 + 2i}; \tag{6}$$

ε_1 and ε_2 are the relative permittivities of the carbon matrix and nanoparticles, respectively; ε_0 is the permittivity of a vacuum; and σ is the specific conductivity of the MFCNT nanocomposite.

The reflection coefficient is determined as

$$R(\omega) = 20\log\left|\frac{Z(\omega) - Z_0}{Z(\omega) + Z_0}\right|; \tag{7}$$

here $Z(\omega) = \sqrt{\mu_0\mu(\omega)/\varepsilon_0\varepsilon(\omega)}$ represents the wave resistance of the nanocomposite and $Z_0 = 377\ \Omega$ is the characteristic impedance of the plane wave in vacuum.

The transmission coefficient determines the screening efficiency and depends on the absorption, reflection, and processes of multiple reflection inside the nanocomposite; it is expressed as

$$T(\omega) = 8,68\,\mathrm{Re}(\gamma) + 20\log\left|\frac{(Z_0 + Z)^2}{4Z_0 Z}\right|$$
$$+ 20\log\left|1 + \exp[-d\,\mathrm{Re}(\gamma)]\frac{(Z_0 - Z)^2}{(Z_0 + Z)^2}\right|, \tag{8}$$

where d is the nanocomposite thickness and $\gamma(\omega) = i\omega\sqrt{\mu_0\mu(\omega)\varepsilon_0\varepsilon(\omega)}$ is the propagation coefficient.

The contour impedance Z_i depends on the contribution of the resonant circuits containing the active resistance R_i, inductance L_i, and capacitance C_i. Its resonant cyclic frequency is $\omega_0 = \sqrt{L_i C_i}$. In the studied MFCNT nanocomposite, in which an arbitrary distribution of resistive, inductive, and capacitive couplings is observed, various types of connections between R_i, L_i, and C_i result in various expressions for the impedance of the contours under consideration.

For a consecutive circuit, the impedance is

$$Z_i = R_i + i\left(\omega L_i - \frac{1}{\omega C_i}\right). \qquad (9)$$

For a partially parallel $R_i L_i C_i$ chain (it is assumed that resistance R_i is connected in series to inductance L_i, and these two elements are connected in parallel to capacitance C_i), the impedance is written as

$$Z_i = \frac{R_i + i\omega L_i}{i\omega C_i\left[R_i + i\left(\omega L_i - \dfrac{1}{\omega C_i}\right)\right]}. \qquad (10)$$

For a series-parallel connection of elements (L_i and C_i are connected in parallel, and R_i is connected in series to them), the impedance is

$$Z_i = R_i + \left[i\omega C_i + \frac{1}{i\omega L_i}\right]^{-1}. \qquad (11)$$

For a completely parallel chain (L_i, C_i, and R_i are connected in parallel to each other), we have

$$Z_i = \left[R_i^{-1} + i\left(\omega C_i - \frac{1}{\omega L_i}\right)\right]^{-1}. \qquad (12)$$

Equations (1), (4), (7), and (8) together with Eqs. (2), (3), (5), (6), and (9)–(12) were used to calculate frequency dependences $\varepsilon(\omega)$, $\mu(\omega)$, $R(\omega)$, and $T(\omega)$. For all results presented in this study, the conductivity $\sigma = 120\ (\Omega\ \mathrm{m})^{-1}$ and the bulk concentration of nanoparticles $N = 0.1$ [3]. As the frequency dependences were calculated, the real frequency $f = \omega/2\pi$ was used instead of a cyclic frequency. In addition, the frequency dependence for the permittivity takes place only for complex component ε'' in simple form ($\varepsilon''(\omega) \sim \sigma/\omega$); therefore, we present no results from analyzing the dependences $\varepsilon(\omega)$.

RESULTS AND DISCUSSION

Series $R_i L_i C_i$ Contour

In this case, the impedance is described by expression (9) and the strong nonlinearity of dependence $\mu(f)$; hence, $R(f)$ and $T(f)$ are obtained near the resonance frequency of the contour. The result is shown in Fig. 2 (curves 1 and 2). In addition, the results of calculations show that a deep gap (Fig. 2a, curves 3 and 4) is formed on dependence $\mu(f)$ at a certain value of the

contour parameters, which results in an appreciable decrease in EMR absorption. In this case, the reflection and transmission coefficients substantially increase (Fig. 2, curves 3 and 4). Hence, the parameters of the $R_i L_i C_i$ contour determine the character of the frequency dependence of coefficients R and T from a smooth broad resonance to their sharp increase at certain frequencies. In the latter case, the resonance is characterized by appreciable steps on dependences $R(f)$ and $T(f)$. So, the values of the reflection coefficient increase from -2 to almost 0 dB, and the transmission coefficient increases from -22 to -10 dB. The step width, as the calculations show, can reach $10-15$ GHz.

It is established that a decrease in the inductance and interface capacitance results in a shift of the resonance towards higher frequencies. An increase in L_i and C_i (or R_i) results in a shift of the resonance frequency towards a lower frequency region, a narrowing of resonance width, and a transition to a broad implicit resonance (see Fig. 2b, curves 1 and 2).

Partially Parallel $R_i L_i C_i$ Contour

It is established that the steps arise at certain parameters of the chain on the frequency dependences of μ, R, and T (Fig. 3). In this case, the real part of the magnetic permeability decreases almost to zero, and its imaginary part becomes negative, which means a weakening of absorbing properties. The reflection coefficient sharply increases almost to 0 dB, and the transmission coefficient increases from -22 to -10 dB. A sharp change in the parameter values is observed in the frequency range of $47.89-47.90$ GHz (see Fig. 3, curves 1 and 2). After this sharp change, all frequency dependences of parameters are weak up to the resonance frequency of the contour. The calculations show that an increase in resistance R_i shifts the frequency of occurrence of a step towards higher values and narrows its width. An increase in inductance or capacitance only weakly affects the frequency at which the step occurs, but causes its narrowing. An increase in R_i to values of $0.05\ \Omega$ or in L_i to $0.08\ \pi\mathrm{H}$ results in smoothing of the frequency dependences of all parameters in the studied frequency range (see Fig. 3, curves 3 and 4).

From the analysis of the results in Fig. 3, it follows that near 50 GHz, a specific resonance, which is not directly associated with the resonance frequency of the $R_i L_i C_i$ contour, is observed and induced by the features of the MFCNT nanocomposite. In this case, the function $Q_\mu(\omega)^2$ shows a local minimum. It means that, for a partially parallel $R_i L_i C_i$ contour, the resonance of the nanocomposite properties is caused both by the resonance of the contour and by the internal resonance of the complex structure of the MFCNT nanocomposite (mainly, its magnetic component).
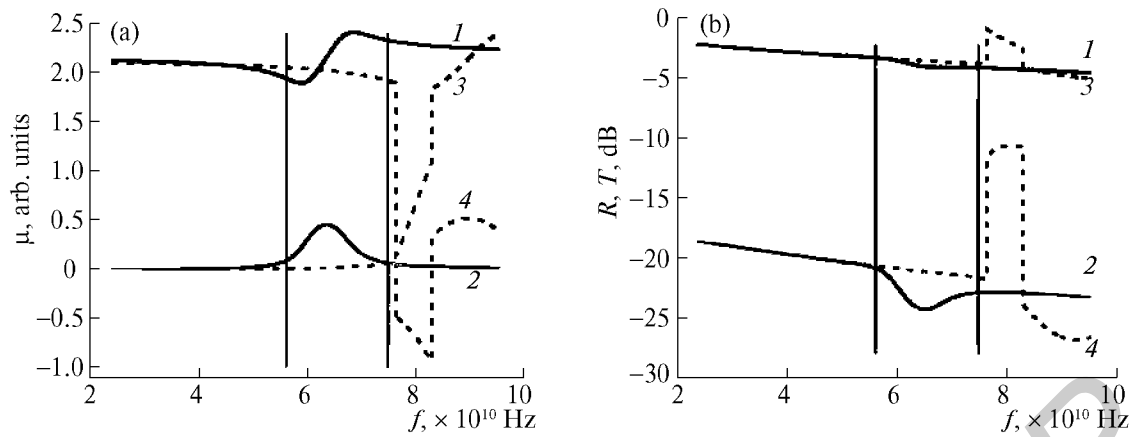
Fig. 2. (a) Frequency dependences of real (curves *1* and *3*) and imaginary (curves *2* and *4*) parts of magnetic permeability and (b) reflection R (curves *1* and *3*) and transmission T (curves *2* and *4*) coefficients of MFCNT nanocomposite for serial $R_i L_i C_i$ contour: *1, 2*—$R_i = 0.012\ \Omega$, $L_i = 0.4\ \pi$H, $C_i = 20\ \pi$F (the resonant frequency $f_0 = 56.3$ GHz); *3, 4*—$R_i = 0.01\ \Omega$, $L_i = 0.25\ \pi$H, $C_i = 18\ \pi$F ($f_0 = 75$ GHz). Resonance frequencies are specified with vertical lines.
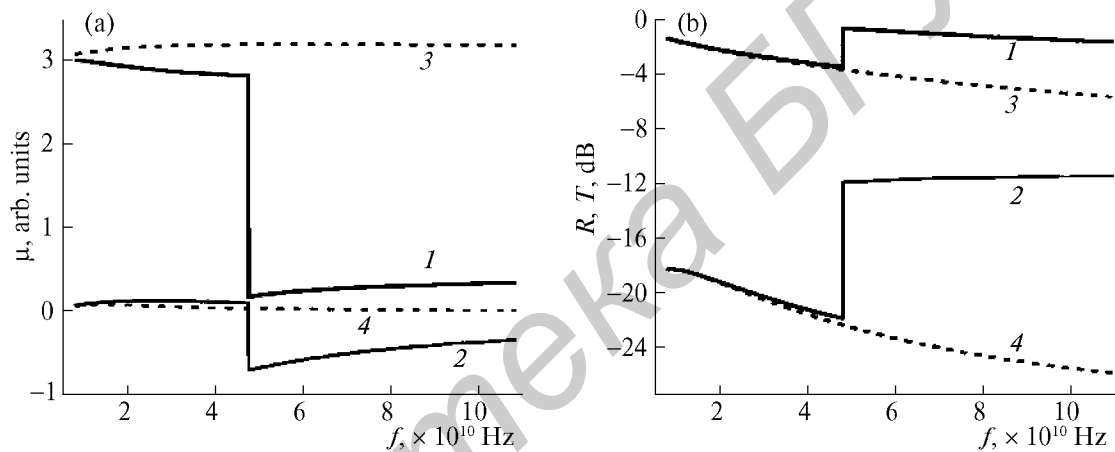
Fig. 3. (a) Frequency dependences of real (curves *1* and *3*) and imaginary (curves *2* and *4*) parts of magnetic permeability and (b) reflection R (curves *1* and *3*) and transmission T (curves *2* and *4*) coefficients of MFCNT nanocomposite for partially parallel $R_i L_i C_i$ contour: *1, 2*—$R_i = 0.01\ \Omega$, $L_i = 0.02\ \pi$H, $C_i = 1\ \pi$F ($f_0 = 1.123$ THz); *3, 4*—$R_i = 0.01\ \Omega$, $L_i = 0.08\ \pi$H, $C_i = 1\ \pi$F ($f_0 = 562$ GHz).

Series–Parallel $R_i L_i C_i$ Contour

It is established that a broad resonance on dependences $\mu(f)$, $R(f)$, and $T(f)$ (Fig. 4, curves *3* and *4*) is observed at frequencies more than 30 GHz farther from resonance frequency f_0. At certain values of R_i, L_i, and C_i, there is a gap of about 40 GHz in width on these dependences, which is distant even farther from the value of f_0 (Fig. 4, curves *1* and *2*). Thus, for the series–parallel contour, two types of resonance are simultaneously observed: a very broad, implicitly expressed resonance and a sharp stepwise resonance with a band to 80 GHz. In this case, the first type of resonance strengthens the absorbing properties of the MFCNT nanocomposite. The second type causes the occurrence of steps on dependences $R(f)$ and $T(f)$: R increases by 2 dB, while T increases by approximately 8 dB, which results in appreciable weakening of EMR absorption. An increase in the nominal value of all three components of the $R_i L_i C_i$ contours results in a decreasing step width and even to its disappearance (see Fig. 4, curves *3* and *4*). This effect arises for the following set of parameters: $R_i = 0.009\ \Omega$, $L_i = 0.08\ \pi$H, and $C_i = 15\ \pi$F. The observable additional resonance is not directly associated with the resonance in a chain and is caused by the complex internal structure of the nanocomposite. In the region of this resonance, the function $Q_\mu(\omega)^2$ has a local peak.
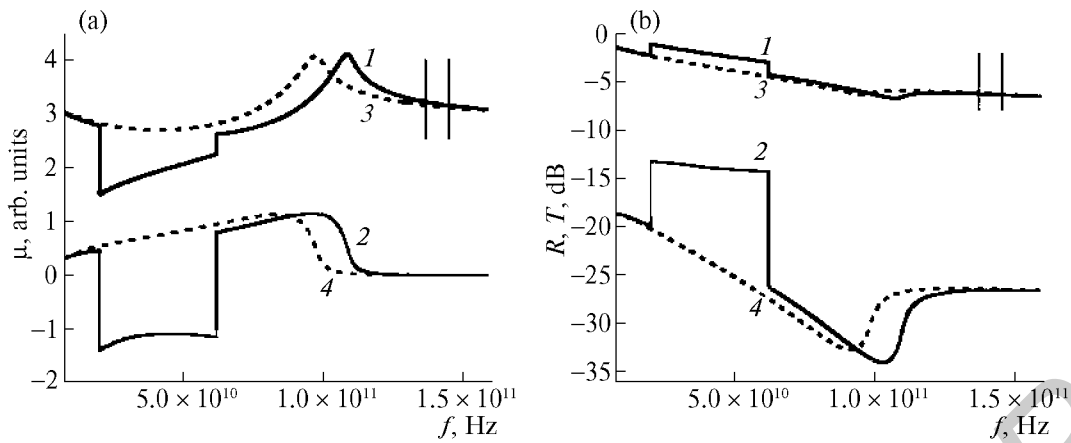
Fig. 4. (a) Frequency dependences of real (curves 1 and 3) and imaginary (curves 2 and 4) parts of the magnetic permeability and (b) reflection R (curves 1 and 3) and transmission T (curves 2 and 4) coefficients of the MFCNT nanocomposite for the series—parallel $R_iL_iC_i$ contour: $1, 2$—$R_i = 0.005\ \Omega$, $L_i = 0.08\ \pi H$, $C_i = 15\ \pi F$ ($f_0 = 145.3$ GHz); $3, 4$—$R_i = 0.005\ \Omega$, $L_i = 0.09\ \pi H$, $C_i = 15\ \pi F$ ($f_0 = 137$ GHz). Resonance frequencies are specified in figure by vertical lines.
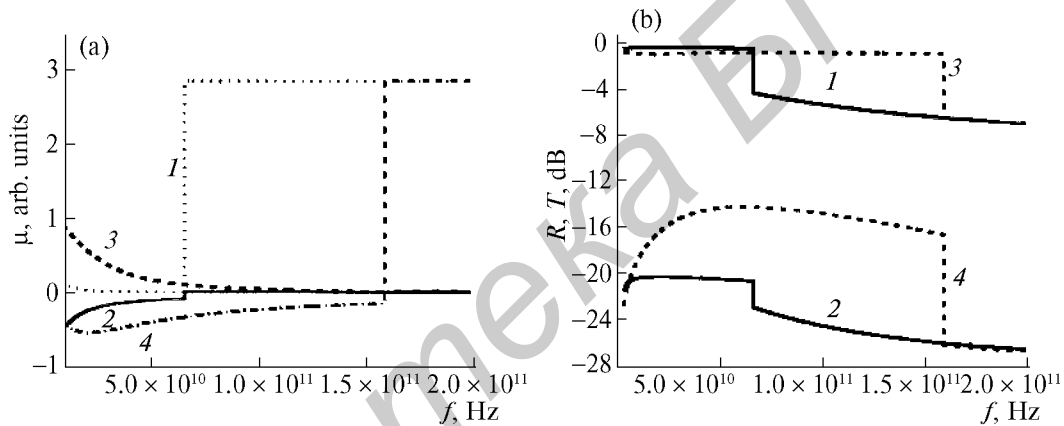
Fig. 5. (a) Frequency dependences of real (curves 1 and 3) and imaginary (curves 2 and 4) parts of magnetic permeability and (b) reflection R (curves 1 and 3) and transmission T (curves 2 and 4) coefficients of MFCNT nanocomposite for completely parallel $R_iL_iC_i$ contour: $1, 2$—$R_i = 0.002\ \Omega$, $L_i = 0.08\ \pi H$, $C_i = 10\ \pi F$ ($f_0 = 172.6$ GHz); $3, 4$—$R_i = 0.009\ \Omega$, $L_i = 0.05\ \pi H$, $C_i = 10\ \pi F$ ($f_0 = 225.1$ GHz).

Completely Parallel $R_iL_iC_i$ Contour

In this case, just like for the partially parallel contour, steps are observed on the dependences $\mu(f)$, $R(f)$, and $T(f)$, (Fig. 5). However, these steps are located inversely with respect to the result shown in Fig. 3; more precisely, there is a strengthening in EMR absorption with increasing frequency. In this case, the real part of the magnetic permeability increases appreciably with frequency (from 0 to 3). The reflection and transmission coefficients sharply decrease. This effect is of interest because it testifies to the possibility of increasing the screening ability of the MFCNT nanocomposite in a wide frequency range.

CONCLUSIONS

The results testify to the prospect of applying MFCNT nanocomposites in the EMR subterahertz range. We will continue to study the absorbing properties of MFCNT nanocomposites in the frequency range to 200 GHz.

REFERENCES

1. R. Saito, G. Dresselhaus, and M. S. Dresselhaus, *Physical Properties of Carbon Nanotubes* (Imperial College Press, London, UK, 1998).

2. J. Federici and L. Moeller, J. Appl. Phys. **107**, 111101 (2010).

3. V. A. Labunov, A. L. Danilyuk, A. L. Prudnikava, et al., J. Appl. Phys. **112**, 024302 (2012).

4. J. Lehman, A. Sers, and L. Hanssen, et al., Nano Lett. **10**, 3261 (2010).

5. S. Rosenblatt, H. Lin, V. Sazonova, et al., Appl. Phys. Lett. **87**, 153111 (2005).

6. I. S. Nefedov, Phys. Rev. B **82**, 155423 (2010).

7. M. S. Dresselhaus, Nature **432** (7020), 959 (2004).

8. A. M. Nemilentsau, G. Ya. Slepyan, and S. A. Maksimenko, Phys. Rev. Lett. **99**, 147403 (2007).

9. P. C. P. Watts, D. R. Ponnampalam, W. K. Hsu, et al., Chem. Phys. Lett. **378**, 609 (2003).

10. A. L. Danilyuk, A. L. Prudnikava, I. V. Komissarov, et al., Carbon **68**, 337 (2014).

Translated by V. Bukhanov

SPELL: OK